Electronic Supplementary Material (ESI) for ChemComm.

A Hexagon Based Mn(II) Rod Metal-Organic Framework – Structure, SF_6 Gas Sorption, Magnetism and Electrochemistry

Francoise M. Amombo Noa,*[a] Ocean Cheung,[b] Michelle Åhlén,[b] Elisabet Ahlberg,[c] Priyanka Nehla,[b] Germán Salazar-Alvarez,[b] Soheil Ershadrad,[d] Biplab Sanyal[d] and Lars Öhrström*

SUPPORTING INFORMATION

Materials and general procedures

All chemicals used for the MOFs synthesis were purchased from Sigma-Aldrich and were used without further purification. The linker 1,2,3,4,5,6-Hexakis(4-carboxyphenyl)benzene (H_6cpb) was purchased from Extension.

Elemental analysis was conducted by Mikroanalytisches Labor Kolbe, c/o Fraunhofer institute, Oberhausen, Germany.

A Mettler Toledo TGA/DSC 3+ star system was used for thermal gravimetric analysis (TGA).

Powder X-ray diffraction (PXRD) patterns were recorded on a Bruker D8 Twin diffractometer (Billerica Massachusetts) with CuKα radiation (λ = 1.54 Å) at room temperature.

Single crystal X-ray diffraction (SCXRD). The MOF CTH-18 data was collected on a Rigaku XtaL AB Synergy-DW diffractometer equipped with a HyPix-Arc 150º detector using CuKα radiation (λ = 1.54184 Å). The data diffraction was acquired and processed with CrysAlisPro software package.[1,2] Direct methods was utilized for CTH-18 and the refinments were established by full-matrix least squares with SHELX-2018/3 [3] using X-seed[4] and Olex2[5] softwares.

Structure drawings, cavity calculations and porosity were obtained with the aid of CrystalMaker as a software.[6]

Topology analysis were done with Systre.[7]

Scanning electron microscopy (SEM) images for CTH-18 were obtained on a Zeiss Merlin Field Emission Scanning Electron Microscope (Oberkichen, Germany), then operated at 1 kV and 50 pA. Before imaging, the samples were pre-sputtered with Ag/Pd..

Gas adsorption isotherms were recorded using a Micromeritics ASAP2020 surface area analyzer (Norcross, GA, USA). Prior to the analyses CTH-18 was pretreated at 250 ºC under dynamic vacuum at 1 x 10^{-4} Pa. Porosity analysis were carried out by recorded sorption isotherms at liquid N_2 temperature for N_2 (-195 ºC) and at -78 ºC for CO_2. N_2, CO_2, CH_4, SF_6 adsorption isotherms were also recorded at 20 ºC. CO_2 heat of adsorption was calculated using CO_2 adsorptions recorded at 0, 10 and 20 ºC.

MOF Synthesis

H_6cpb (16 mg, 0.020 mmol) and $MnCl_2 \cdot 4H_2O$ (7.94 mg, 0.040 mmol) in a mixture of 2 ml N,N-Dimethylformamide (dmf) and 2 ml glacial acetic acid (*v*/*v*) were added into a pyrex tube and heated at 120 ºC in an oven. After 3 days, the mixture yielded colorless crystals, then the product was filtered off, washed with dmf and left to dry at room temperature. Elementary analysis $C_{57}H_{45}N_3O_{15}Mn_3$ calculated (found): C 58.18 (56.79); H, 3.85 (3.87); N, 3.57 (3.47). Contents of dmf solvent was calculated to 19% and solid MnO_2 residue after TGA in air to 22%. Found by TGA (Figure S10) 19% and 18% respectively.

Table S1. Crystallographic data and structure refinement parameters for CTH-18

Code	CTH-18
Structural formula	$C_{57}H_{45}N_3O_{15}Mn_3$
Molecular mass (g mol^{-1})	1176.78
Data collection temp. (K)	100.00 (10)
Crystal system	Monoclinic
Space group	$P2_1/c$
a (Å)	11.5886(2)
b (Å)	27.8179(4)
c (Å)	16.6789(3)
α (°)	90
β (°)	101.990 (2)
γ (°)	90
Volume ($Å^3$)	5259.48(16)
Z	4
Dc, calc density (g cm^{-3})	1.486
Absorption coefficient (mm^{-1})	6.391
θ range	3.14-75.66
Reflections collected	48937
No data I >2 sigma (*I*)	9060
Final *R* indices [I >2 sigma (*I*)]	R_1 = 0.1176 wR_2 = 0.3164
R indices (all data)	R_1 = 0.1270 wR_2 = 0.3216
Goodness-of-fit on F^2	1.051
CCDC no.	2226584

Figure S1 Asymmetric unit of CTH-18

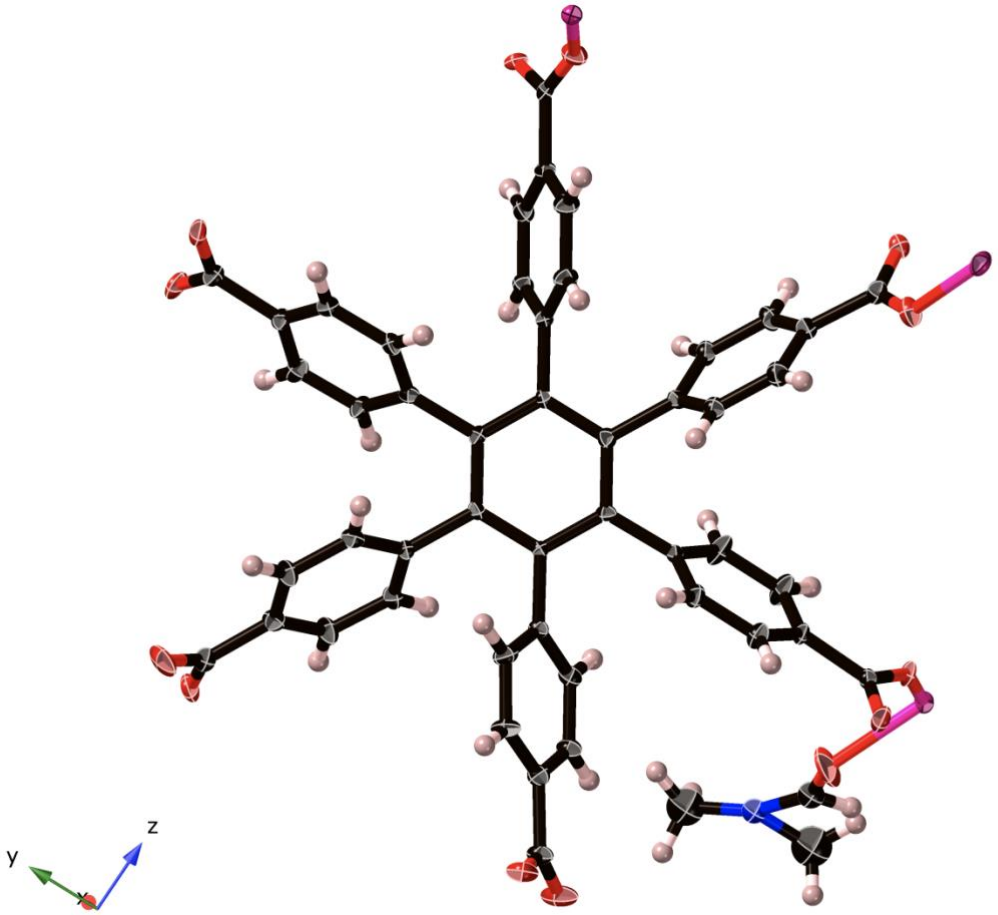

One of several disordered dimethylformamide molecules shown.

Figure S2. Pores size analysis and a tentative explanation of the different pore sizes observed

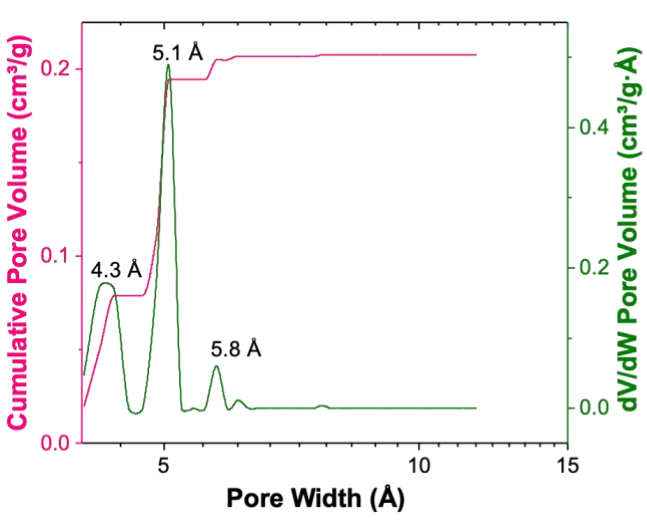

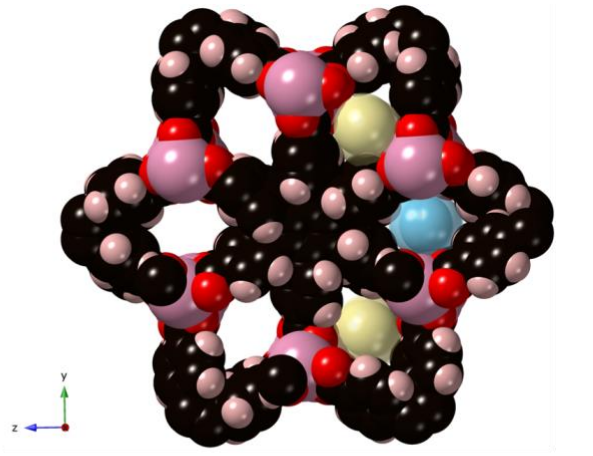

Space filling plot using van der Waals radii and spheres fitted to the two different kinds of voids

In Figure S2 we display how Crystal Maker was used to fit spheres into the empty space of the MOF (dmf molecules having been deleted) Yellow spheres diameter 4.9 Å, blue spheres diameter 4.3 Å

Figure S3. Additional gas sorption figures

Top left. CO_2 adsorption isotherms of **CTH-18** recorded at 0, 10 and 20 °C (top to bottom). Top right. Isosteric heat of CO_2 adsorption vs loading calculated using the Clapeyron–Clausius equation. Bottom left, water adsorption/desorption isotherms of **CTH-18** recorded at 20 °C. Bottom right SF_6 adsorption kinetics on **CTH-18**, up to 80% (over 11.2 wt.%) of the equilibrium uptake was reached within 600 seconds (equilibrium time = 1h).

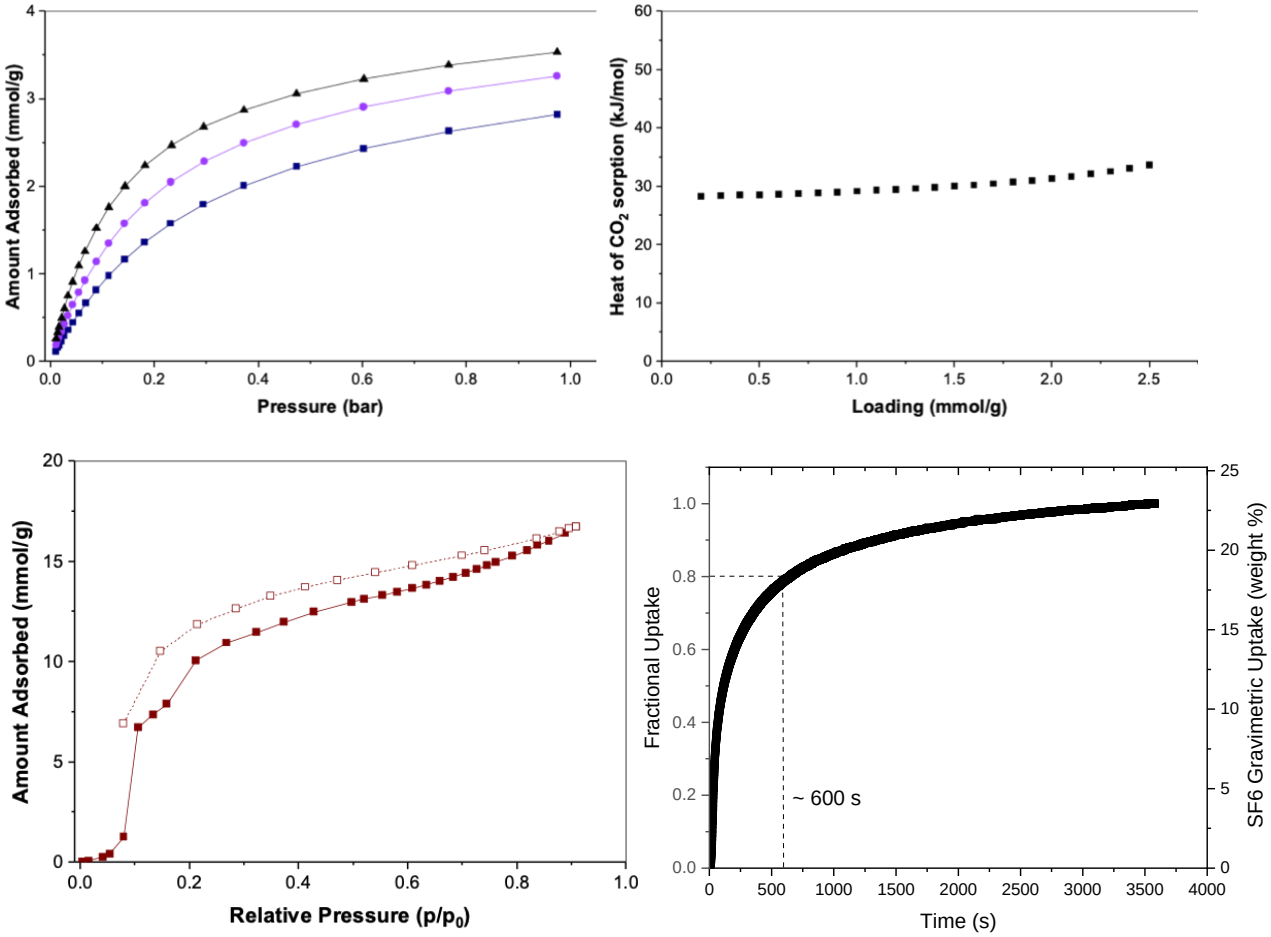

Figure S4. High cyclic SF_6 uptake stability

Top left: Nitrogen adsorption isotherms of **CTH-18** after 4 SF_6 vacuum swing adsorption/desorption cycles (VSA) and after 10 temperature swing adsorption/desorption cycles (TSA). The CTH-18 samples were pretreated at 250°C under dynamic vacuum at 1 x 10^{-4} Pa before the N_2 sorption measurements. The BET and Langmuir surface area of the VSA sample were 291 and 361 , and for the TSA sample, 291 and 367 m^2/g, respectively. Top right: SF_6 adsorption isotherm of **CTH-18** recorded at 20, 25 and 30° C (top to bottom). Bottom left: Isosteric heat of SF_6 adsorption vs loading calculated using the Clapeyron-Clausius equation. Bottom right: Cyclic SF_6 relative uptake on **CTH-18** when sample was only regenerated using vacuum (vacuum swing adsorption), between cycle 3 and 4 the sample was heated to 250°C for 10 minutes for regeneration. The decrease in relative uptake between cycle 1 and 2 was related to a small amount of SF_6 that could not be desorbed from **CTH-18** due to the narrow pore size of CTH-18, heat regeneration was able to recovered all the SF_6 uptake capacity (between cycle 3 and 4).

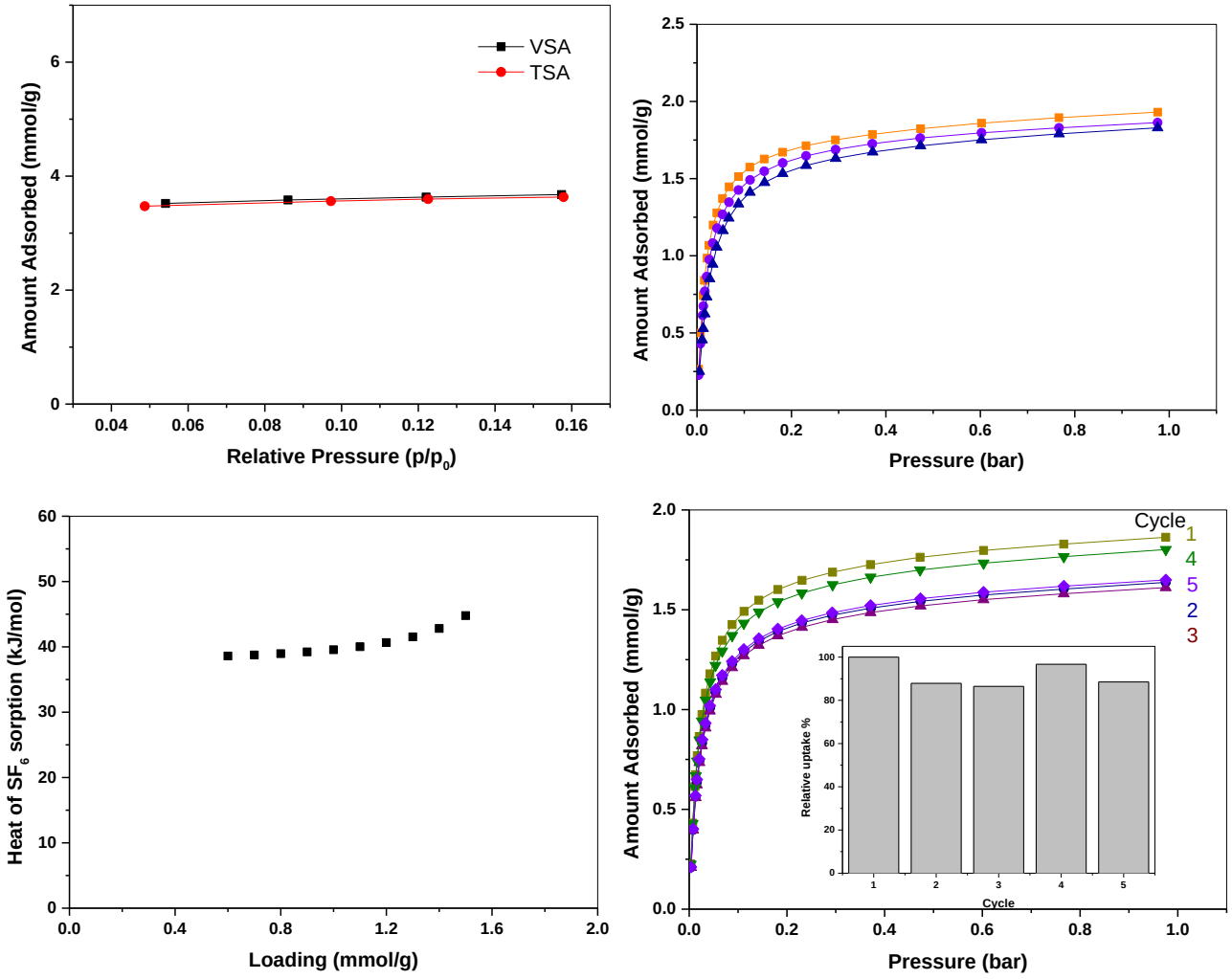

Figure S5. Field dependence of the magnetization for CTH-18.

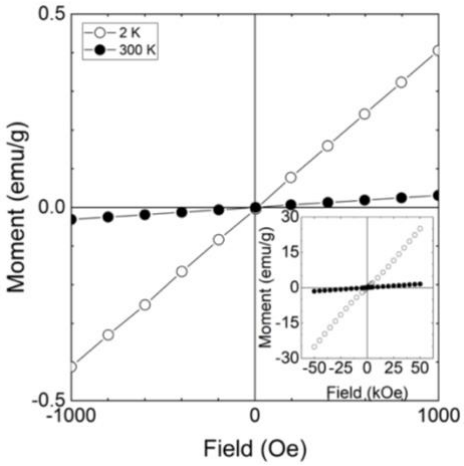

Quasistatic DC magnetic measurements were performed using a Quantum Design superconducting quantum interference device (SQUID) MPMS XL magnetometer. Magnetisation versus temperature studies were carried out using a 1 kOe field. About 16 mg of the powder were packed in a gel capsule and mounted on a plastic straw. The diamagnetic contribution of the sample holder was removed from the signal.

Electrochemistry

Simulations of the voltammetric response were made using the Gamry DigiElch software. Initially an electron transfer for Mn(II)-MOF ↔ Mn(III)-MOF + e^- was tested but is was not possible to reproduce the experimental voltammogram. A mechanism separating the electrochemical oxidation and reduction steps was necessary to get a reasonable fit to the experimental data. The oxidation reaction is coupled with a fast chemical reaction, where an anion becomes associated with the active site. This complex is then reduced on the negative going scan and the anion leaves. The parameters were optimised for the voltammogram at 2 Vs^{-1} and then used for all other sweep rates. The comparison with experimental data shows that other processes are involved as well.

Figure S6. Simulated cyclic voltammograms at different sweep rates, see figure legends.

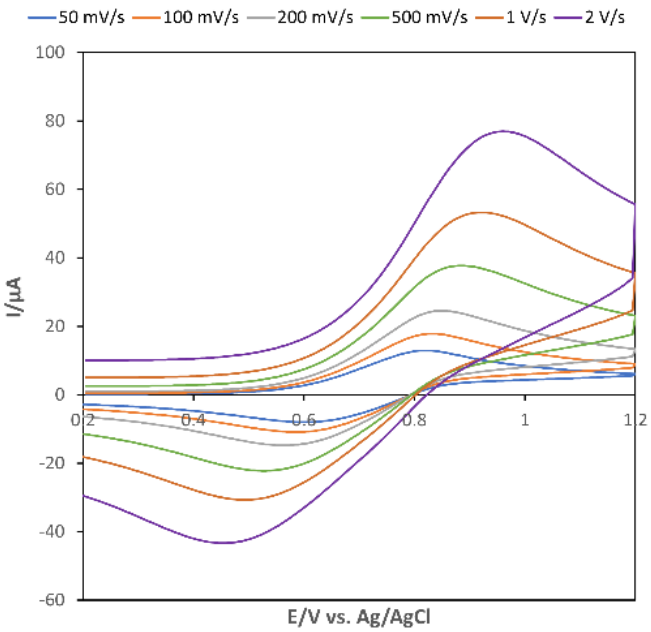

Extending the potential to 1.5 V vs. Ag/AgCl show an increase in current. This can be due to oxygen evolution or oxidation of the MOF.

Figure S7. Cyclic voltammetry at 500 mV/s in phosphate buffer pH = 7

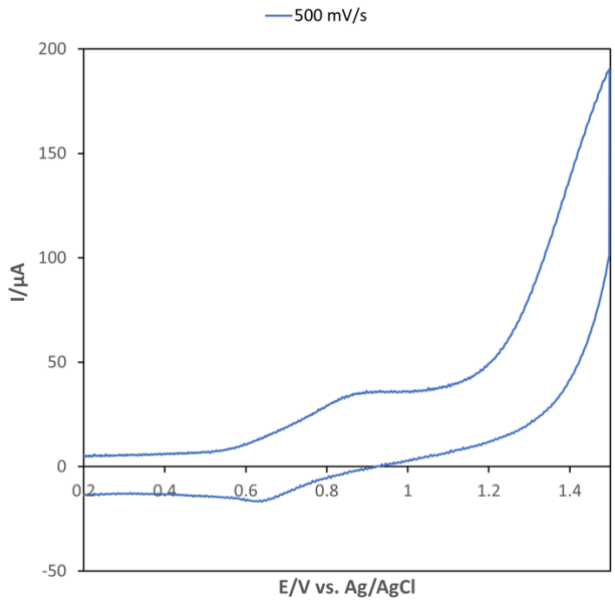

Figure S8 The cpb linkers are stacked with spacing 5.7 Å and adjacent linkers have opposite conformational chirality.

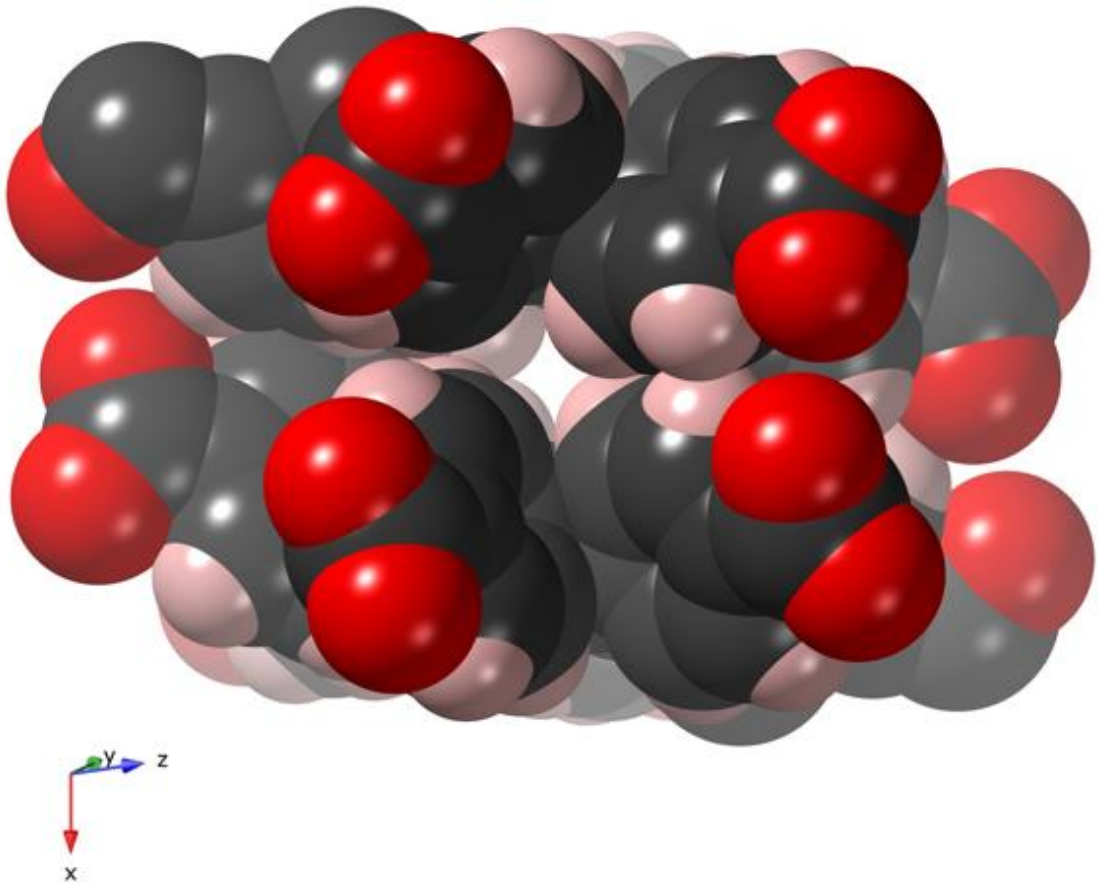

Figure S9 Network topology analysis

Left: The straight rod, STR, approach giving a three nodal 4- and 6-connected net with point symbol $\{5^2.6^3.7\}\{4.5^2.6^2.7\}\{4.5^4.6^6.7^4\}$. Right: The point-of-extension method giving a four-nodal six-connected net with point symbol $3\{3^6.4^4.6^5\}\{6^{11}.7^4\}$

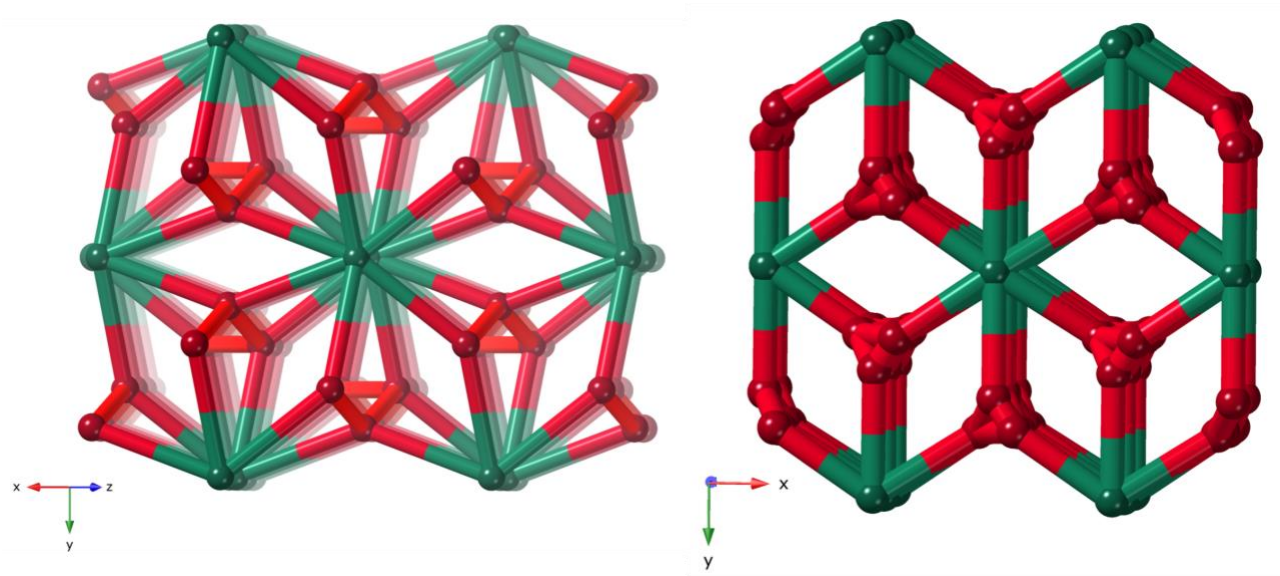

Computational methods

A plane-wave basis set with an energy cutoff of 400 eV was used to perform first principles calculations based on density functional theory (DFT). Projector augmented wave potentials[8] were used, and the exchange-correlation potential was approximated by a generalized gradient approximation (GGA) using the Perdew, Burke, and Ernzerhof (PBE) functional.[9] Brillouin zone integration was done using the Gamma point. We took the energy convergence criterion between two consecutive electronic steps to be 10^{-5} eV. All calculations were performed using the Vienna Ab initio Simulation Package (VASP).[10]

SYSTRE input and output files

Input Straight rod (STR)

```
CRYSTAL
  NAME MnH6
  GROUP P21/c
  CELL 11.5886 27.8179 16.6789 90.0000 101.990 90.0000
  NODE 1 6 0.75 0.50 0.50
EDGE 1 0.9393 0.8288 0.4813
EDGE 1 0.9393 0.6712 0.9813
EDGE 1 0.7151 0.3312 0.9870
EDGE 1 0.7151 0.1688 0.4870
EDGE 1 0.3906 0.3447 0.0028
EDGE 1 0.6094 0.6553 -0.0028
  NODE 2 4 0.7151 0.3312 0.9870
EDGE 2 1.0607 0.3288 1.0187
EDGE 2 0.3906 0.3447 1.0028
  NODE 3 4 0.9393 0.6712 0.9813
EDGE 3 1.2849 0.6688 1.0130
EDGE 3 0.6094 0.6553 0.9972
  NODE 4 4 0.3906 0.3447 0.0028
END
```

Output Straight rod (STR)

```
Structure #1 - "MnH6".
   Input structure described as 3-periodic.
   Given space group is P21/c.
   16 nodes and 36 edges in repeat unit as given.
   Ideal repeat unit smaller than given (18 vs 36 edges).
   Point group has 4 elements.
   3 kinds of node.
   Equivalences for non-unique nodes:
      3 --> 2
   Coordination sequences:
      Node 4:    4 15 40 69 114 155 226 279 364 447
      Node 2:    4 16 41 71 112 160 219 285 365 446
      Node 1:    6 17 41 73 111 165 216 291 361 448
   TD10 = 1721
   Wells point symbols:
      Node 4:   4.5^2.6^2.7
      Node 2:   5^2.6^3.7
      Node 1:   4.5^4.6^6.7^4
   Ideal space group is C12/m1.
   Ideal group or setting differs from given (C12/m1 vs P121/c1).
   Structure is new for this run.
   Relaxed cell parameters:
       a = 2.08902, b = 3.11525, c = 2.69778
       alpha = 90.0000, beta = 110.2738, gamma = 90.0000
   Cell volume: 16.46900
   Relaxed positions:
      Node 4:    0.00000 0.11206 0.00000
      Node 2:    0.41451 0.19944 0.30244
      Node 1:    0.74127 0.00000 0.22271
   Edges:
      0.74127 0.00000 0.22271  <->  0.91451 0.30056 0.30244
      0.00000 0.11206 0.00000  <->  0.41451 0.19944 0.30244
      0.41451 0.19944 0.30244  <->  0.58549 0.19944 0.69756
      0.00000 0.11206 0.00000  <->  0.25873 0.00000 -0.22271
      0.74127 0.00000 0.22271  <->  0.41451 0.19944 0.30244
   Edge centers:
      0.82789 0.15028 0.26257
      0.20725 0.15575 0.15122
      0.50000 0.19944 0.50000
      0.12936 0.05603 -0.11135
      0.57789 0.09972 0.26257
   Edge statistics: minimum = 0.99999, maximum = 1.00001, average = 1.00000
   Angle statistics: minimum = 40.86198, maximum = 153.82556, average = 107.43840
   Shortest non-bonded distance = 0.69816
   Degrees of freedom: 10
Finished structure #1 - "MnH6".
```

Input Points of extension

```
CRYSTAL
  NAME MnH6
  GROUP C2/m
  CELL 2.51255 4.60549 1.45152 90.0000 93.1633 90.0000
  NODE 2 6  0.02856 0.29137 0.34395
  NODE 4 6  0.19349 0.13575 0.01058
  NODE 6 6  0.33505 0.39120 0.30970
  NODE 1 6  0.49709 0.00000 0.15756
  EDGE  0.02856 0.29137 0.34395   0.16495 0.10880 0.69030
  EDGE  0.49709 0.00000 0.15756   0.83505 0.10880 0.30970
  EDGE  0.19349 0.13575 0.01058   0.16495 0.10880 0.69030
  EDGE  0.19349 0.13575 0.01058   -0.02856 0.29137 -0.34395
  EDGE  0.49709 0.00000 0.15756   0.52856 0.20863 0.34395
  EDGE  0.19349 0.13575 0.01058   -0.16495 0.10880 0.30970
  EDGE  0.02856 0.29137 0.34395   -0.02856 0.29137 -0.34395
  EDGE  0.33505 0.39120 0.30970   0.66495 0.39120 0.69030
  EDGE  0.49709 0.00000 0.15756   0.19349 0.13575 0.01058
  EDGE  0.19349 0.13575 0.01058   -0.19349 0.13575 -0.01058
  EDGE  0.02856 0.29137 0.34395   -0.16495 0.10880 0.30970
  EDGE  0.19349 0.13575 0.01058   0.02856 0.29137 0.34395
END
```

Output Points of extension

```
   Input structure described as 3-periodic.
   Given space group is C2/m.
   14 nodes and 42 edges in repeat unit as given.
   Given repeat unit is accurate.
   Point group has 4 elements.
   4 kinds of node.
   Coordination sequences:
      Node 2:    6 14 53 92 112 209 273 307 467 540
      Node 4:    6 14 51 92 112 209 270 307 468 539
      Node 6:    6 14 51 91 115 206 270 307 470 541
      Node 1:    6 30 38 83 168 161 260 401 366 552
   TD10 = 2071
   Wells point symbols:
      Node 2:   3^6.4^4.6^5
      Node 4:   3^6.4^4.6^5
      Node 6:   3^6.4^4.6^5
      Node 1:   6^11.7^4
   Ideal space group is C12/m1.
   Structure is new for this run.
   Relaxed cell parameters:
       a = 2.77777, b = 3.34746, c = 1.48533
       alpha = 90.0000, beta = 90.9549, gamma = 90.0000
   Cell volume: 13.80934
   Relaxed positions:
      Node 2:    0.04169 0.20696 0.35984
      Node 4:    0.31113 0.42834 0.09512
      Node 6:    0.12184 0.07166 0.31475
      Node 1:    0.47290 0.00000 0.26926
   Edges:
      0.12184 0.07166 0.31475  <->  0.04169 -0.20696 0.35984
      0.12184 0.07166 0.31475  <->  -0.04169 -0.20696 0.64016
      0.47290 0.00000 0.26926  <->  0.54169 0.29304 0.35984
      0.31113 0.42834 0.09512  <->  0.68887 0.42834 -0.09512
      0.04169 0.20696 0.35984  <->  -0.18887 0.07166 0.09512
      0.47290 0.00000 0.26926  <->  0.12184 0.07166 0.31475
      0.12184 0.07166 0.31475  <->  -0.18887 -0.07166 0.09512
      0.12184 0.07166 0.31475  <->  -0.12184 0.07166 0.68525
      0.12184 0.07166 0.31475  <->  0.18887 -0.07166 0.90488
      0.04169 0.20696 0.35984  <->  -0.04169 0.20696 -0.35984
      0.04169 0.20696 0.35984  <->  0.18887 0.07166 -0.09512
      0.47290 0.00000 0.26926  <->  0.81113 0.07166 0.09512
   Edge centers:
      0.08177 -0.06765 0.33729
      0.04007 -0.06765 0.47745
      0.50730 0.14652 0.31455
      0.50000 0.42834 0.00000
      -0.07359 0.13931 0.22748
      0.29737 0.03583 0.29200
      -0.03351 -0.00000 0.20493
      -0.00000 0.07166 0.50000
      0.15535 -0.00000 0.60982
      0.00000 0.20696 0.00000
      0.11528 0.13931 0.13236
      0.64202 0.03583 0.18219
   Edge statistics: minimum = 0.87266, maximum = 1.14769, average = 1.00000
   Angle statistics: minimum = 24.30140, maximum = 168.96240, average = 88.20087
```

```
Shortest non-bonded distance = 0.47977
Degrees of freedom: 15
```

Figure S10. Scanning Electron Microscopy (SEM)

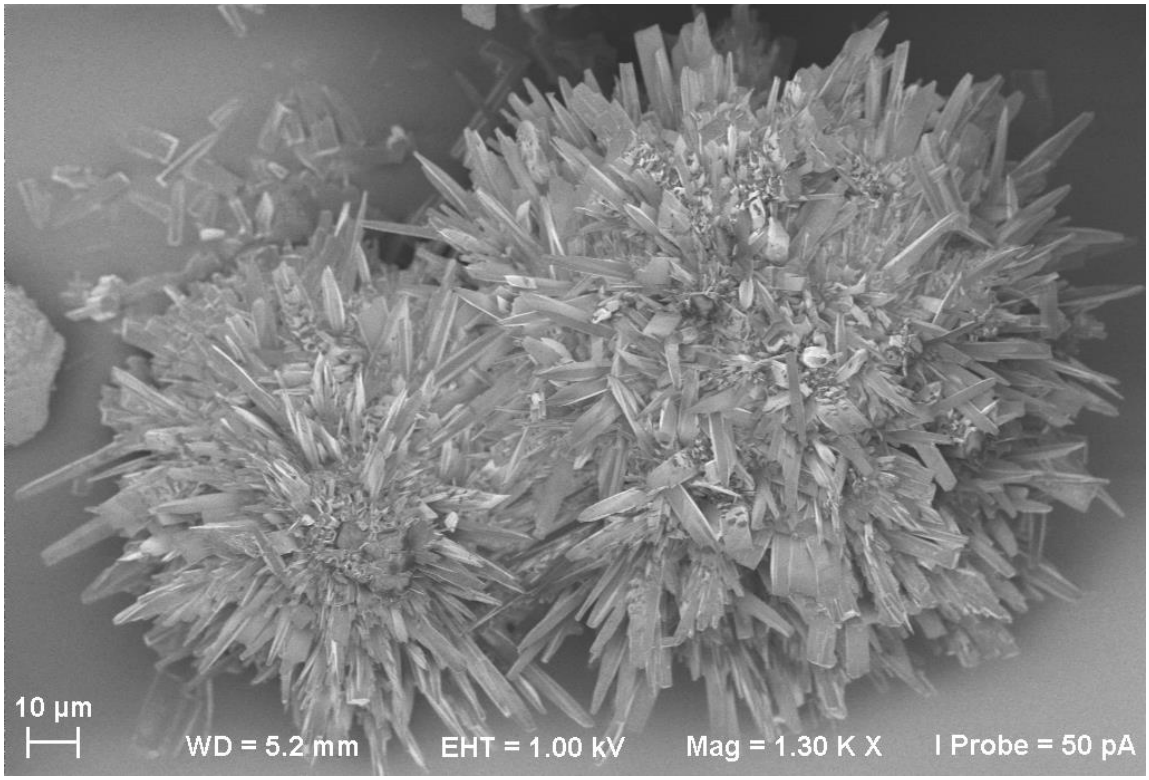

Figure S11. Thermal Analysis

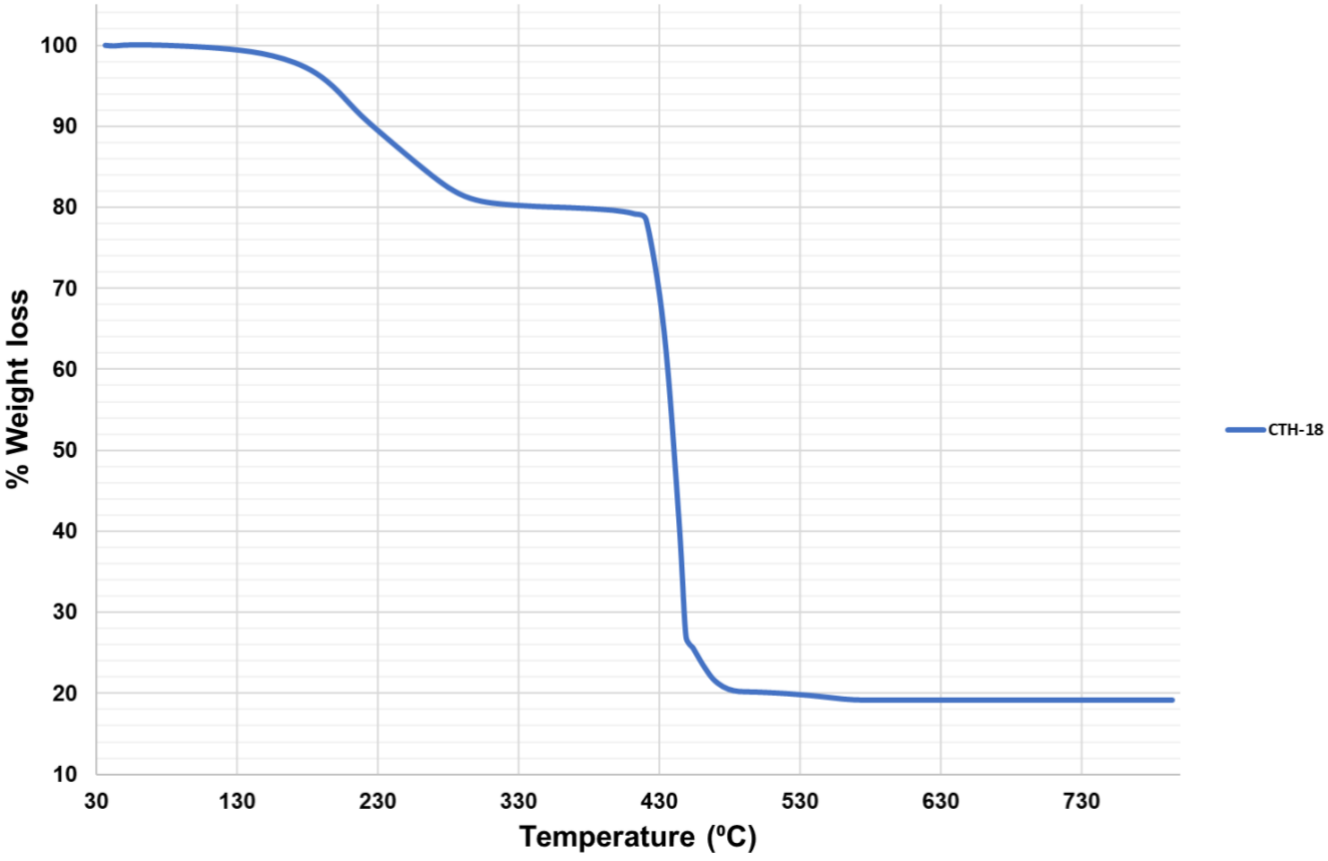

Figure S12. PXRD

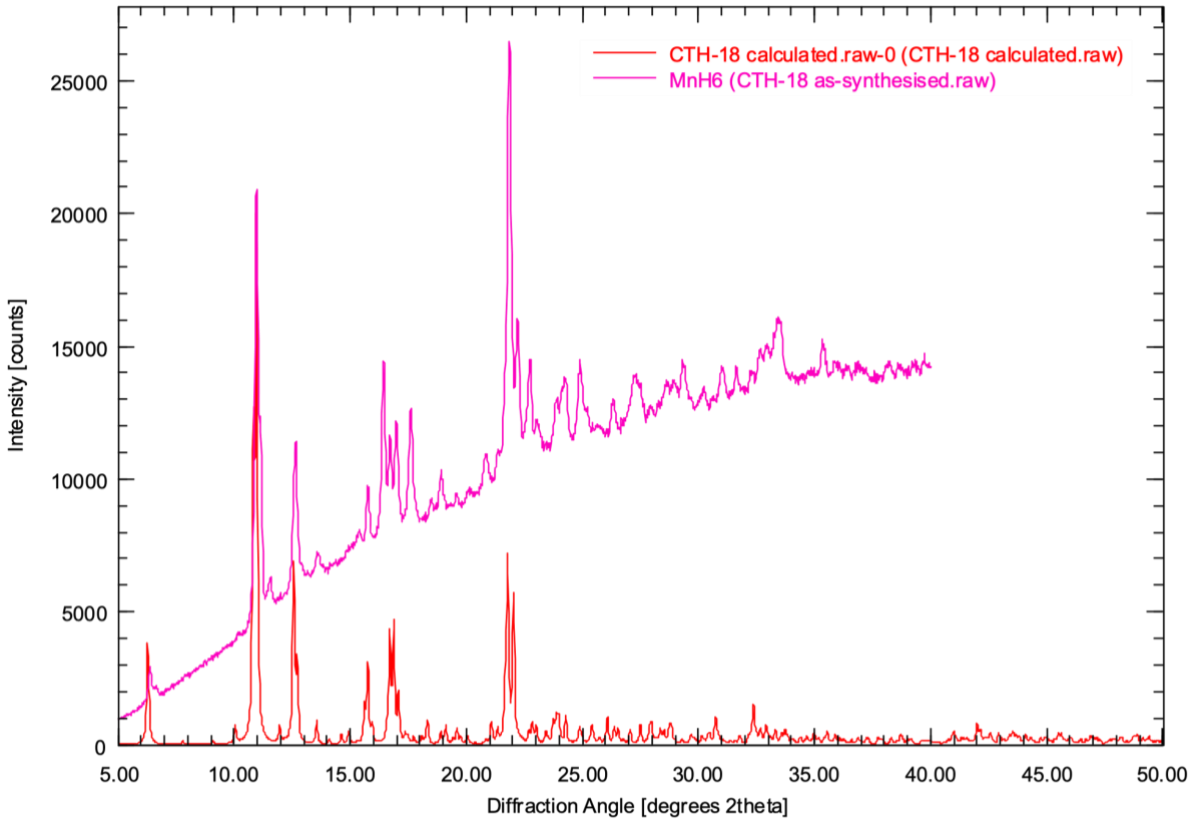

Figure S13. Chemical Stability

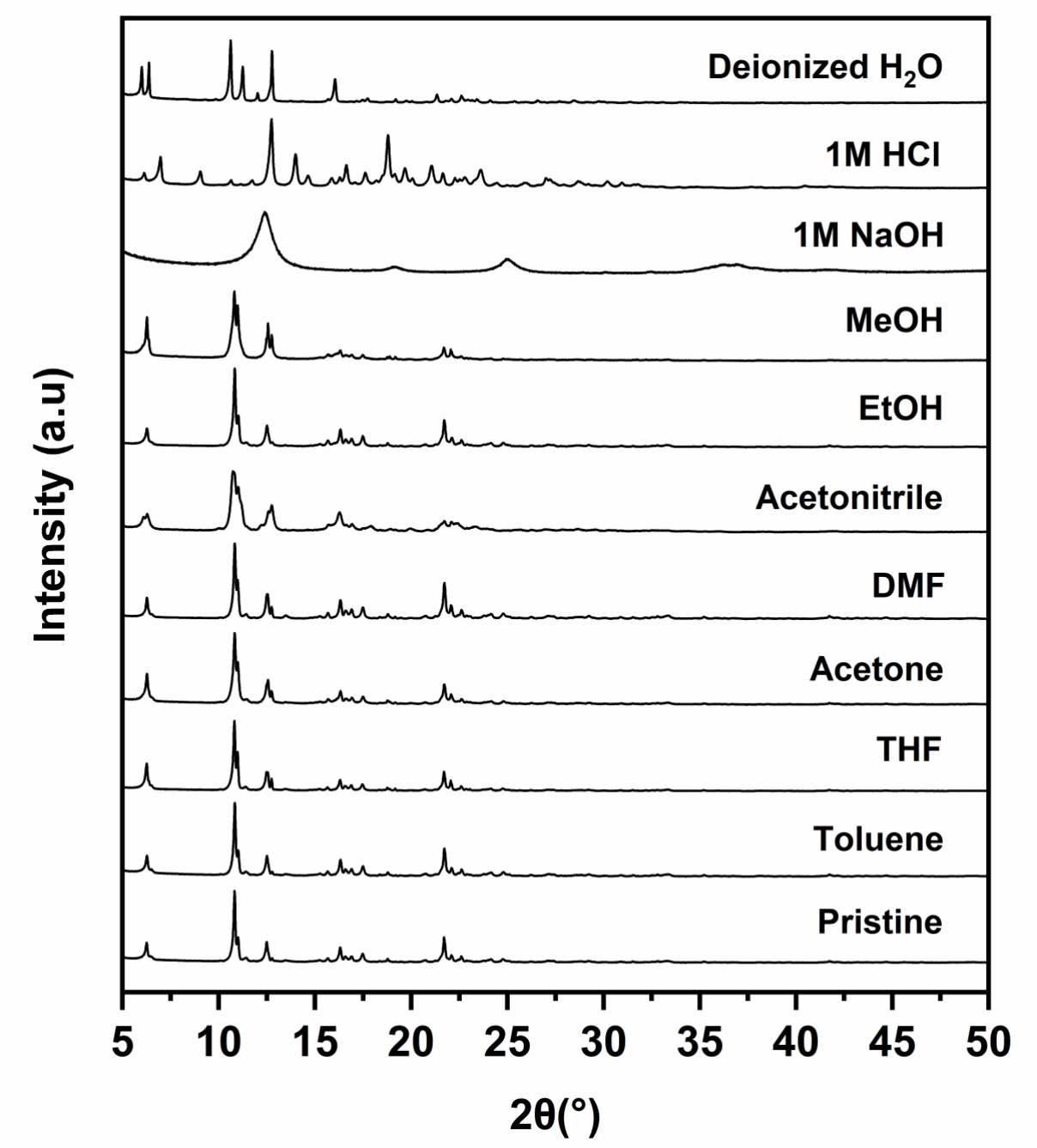

References

1. Crysalis CCD; Oxford Diffraction Ltd: Abingdon, Oxfordshire, UK, 2005.
2. Crysalis RED; Oxford Diffraction Ltd: Abingdon, Oxfordshire, UK, 2005.
3. Sheldrick, G. M. Crystal structure refinement with SHELXL. Acta Crystallogr., Sect. C: Struct. Chem. 2015, 71, 3– 8.
4. Barbour, L. J. X-Seed 4: updates to a program for small-molecule supramolecular crystallography. J. Appl. Crystallogr. 2020, 53, 1141– 1146.
5. Dolomanov, O. V.; Bourhis, L. J.; Gildea, R. J.; Howard, J. A. K.; Puschmann, H. OLEX2: a complete structure solution, refinement and analysis program. J. Appl. Crystallogr. 2009, 42, 339– 341.
6. Images and video generated using CrystalMaker®: a Crystal and Molecular Structures Program for Mac and Windows; CrystalMaker Software Ltd: Oxford, England www.crystalmaker.com, 2019.
7. Delgado-Friedrichs, O.; O'Keeffe, M. Identification and symmetry computation for crystal nets. Acta Crystallogr., Sect. A: Found. Crystallogr. 2003, 59, 351– 360.
8. Blöchl, P. E. Projector augmented-wave method. Phys. Rev. B 1994, 50, 17953.
9. Perdew JP, Burke K, Ernzerhof M. Generalized gradient approximation made simple. Phys. Rev. Lett. 1996, 77, 3865.
10. Kresse G, Furthmüller J. Efficient iterative schemes for ab initio total-energy calculations using a plane-wave basis set. Phys. Rev. B 1996, 54, 11169.